CHEMICAL PHYSICS

Spatial localization of charged molecules by salt ions in oil-confined water microdroplets

SangMoon Lhee[1]*, Jae Kyoo Lee[2]*, Jooyoun Kang[1,2], Shota Kato[1], Sunhee Kim[1], Richard N. Zare[2†], Hong Gil Nam[1,3†]

Copyright © 2020 The Authors, some rights reserved; exclusive licensee American Association for the Advancement of Science. No claim to original U.S. Government Works. Distributed under a Creative Commons Attribution NonCommercial License 4.0 (CC BY-NC).

Cells contain more than 100 mM salt ions that are typically confined to dimensions of 5 to 10 micrometers by a hydrophobic cellular membrane. We found that in aqueous microdroplets having the same size as cells and that are confined in hydrocarbon oil, negatively charged molecules were distributed rather uniformly over the interior of the microdroplet, whereas positively charged molecules were localized at and near the surface. However, the addition of salt (NaCl) to the microdroplet caused all charged molecules to be localized near the oil-water interface. This salt-induced relocalization required less salt concentration in microdroplets compared to bulk water. Moreover, the localization became more prominent as the size of the microdroplet was reduced. The relocatization also critically depended on the type of oil. Our results imply that salt ions and different hydrophobic interfaces together may govern the local distribution of charged biomolecules in confined intracellular environments.

INTRODUCTION

In cells, biomolecular reactions that govern cellular functions and regulations occur in aqueous solution that is confined within a micrometer-sized volume. Behaviors of molecules and chemical reactions, including reaction kinetics, thermodynamics, and redox reactions in micrometer-sized water droplets are distinctively different from those in bulk water, as evidenced by several studies of "microdroplet chemistry" (*1*–*13*). Furthermore, charged molecules are heterogeneously distributed in aqueous microdroplets; fluorescent rhodamine 6G dye molecules are localized and aligned near the water-oil interface of aqueous microdroplets (*14*). This ordered state of molecules near the oil-water interface can increase the collision frequency and lower an entropic barrier during a chemical reaction; therefore, it may provide, in part, a clue for the molecular mechanism of unusual properties observed in microdroplets.

Several previous studies showed distinct behaviors of water and solute molecules at heterogeneous interfaces, including changes in tetrahedral structures of water (*15*) and hydrogen bonding strength (*16*) near surfaces. Ball (*17*) suggested that the water at the surface is more structured and more reactive at interfaces than bulk solution. These studies on these interfacial effects, which are often conducted with different spectroscopic techniques, focus on the surface phenomena occurring within a few nanometer range. Therefore, an overall long-range distribution of molecules beyond the immediate surface has not been well characterized, especially in confined environments.

In addition to the presence of various heterogeneous interfaces in cells, the intracellular aqueous solution contains salt ions at concentrations ranging from 75 to 150 mM. In addition to the effect of salts on various properties of biochemical reactions, including kinetics, thermodynamics, molecular orientation, and enzyme activities (*18*, *19*), salt ions strongly influence the solubility and the aggregation of solutes through the interaction and competition between water molecules and salt ions, called the salting-in or salting-out effect (*20*, *21*). In addition, salt ions induce the adsorption and desorption of solutes to surfaces (*22*, *23*), which can influence the distribution (*24*) and function of biological molecules (*25*). These facts motivated us to explore the effect of salt ions on the distribution of molecules in water microdroplets containing salt ions, inspired by the observation that microdroplets are a good mimic of the intracellular environment (*26*).

We investigate the effect of salt ions on a long-range distribution of molecules by imaging charged water-soluble fluorescent dyes or biological molecules tagged with fluorescent dyes, in water microdroplets enclosed by hydrophobic oil. In the present studies, we address these questions: (i) how salt ions influence the distribution of molecules that have charges near hydrophobic-hydrophilic interfaces beyond the immediate surface, (ii) how salt-induced effects differ in microdroplets compared to bulk solution, and (iii) how different types of interfaces influence the distribution of molecules.

RESULTS AND DISCUSSION

Salt-induced relocalization of charged dyes in microdroplets

We prepared oil-confined aqueous microdroplets by sonicating a 1:10 (v/v) mixture of aqueous solution and hydrocarbon immersion oil in a bath sonicator (*26*). This preparation produced oil-confined microdroplets with sizes ranging from a few to tens of micrometers in diameter (Fig. 1), which was suitable for observing molecular localization. To monitor the molecular localization in water microdroplets confined in oil, we used the fluorescent dyes, MitoTracker Red FM (MitoTracker) and Alexa Fluor 647 (AF647), which have a single positive net charge and three negative charges at neutral pH, respectively (Fig. 1, A and B). We imaged microdroplets containing each dye with a confocal microscope (fig. S1A). To avoid any interference originated from the glass surface, we imaged water microdroplets floating in oil at least 10 μm above the glass surface. The dye distribution depended on the charge on the dye: Positively charged dye molecules gathered near the surface and negatively charged dye molecules appear nearly evenly spread in the interior of a microdroplet. This observation suggests the presence of a negative net charge at the water-oil interface of microdroplets, which result from the preferential adsorption of hydroxide ions or other trace

[1]Center for Plant Aging Research, Institute for Basic Science, Daegu 42988, Republic of Korea. [2]Department of Chemistry, Stanford University, Stanford, CA 94305, USA. [3]Department of New Biology, DGIST, Daegu 42988, Republic of Korea.
*These authors contributed equally to this work.
†Corresponding author. Email: nam@dgist.ac.kr (H.G.N.); zare@stanford.edu (R.N.Z.)

Downloaded from http://advances.sciencemag.org/ on December 29, 2020

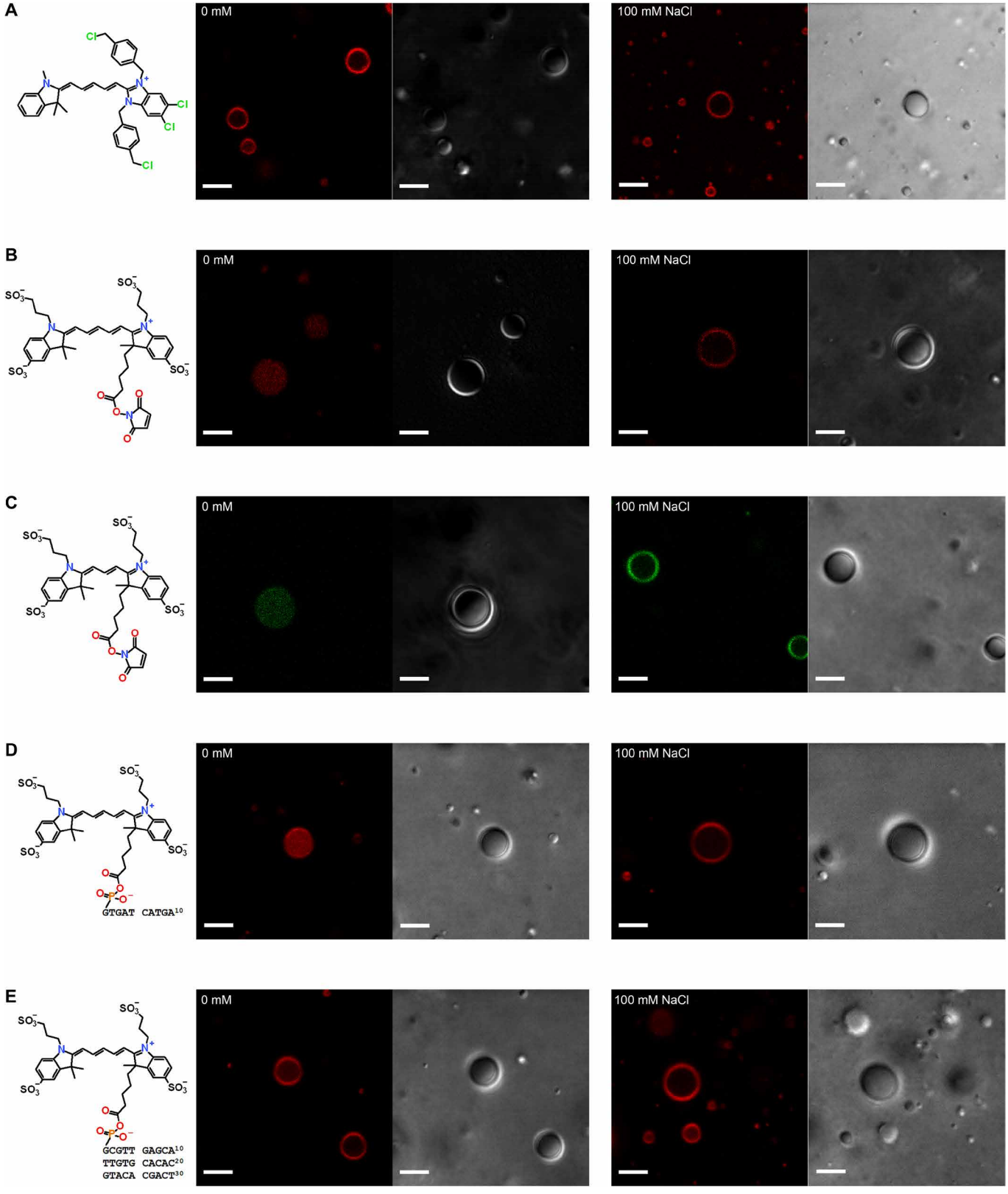

Fig. 1. Spatial distributions of the fluorescent dyes. (**A**) MitoTracker Red FM (MitoTracker), (**B**) Alexa Fluor 647 (AF647), (**C**) Alexa Fluor 555 (AF555), (**D**) 10-bp DNA-AF647, and (**E**) 30-bp DNA-AF647 in aqueous microdroplets suspended in hydrocarbon immersion oil. The chemical structures of the fluorescent dyes with their charges are provided in the left panels, and fluorescence and bright-field images in the absence of salt ions and in the presence of 100 mM NaCl are presented in the middle and right panels, respectively (scale bars, 5 μm).

Downloaded from http://advances.sciencemag.org/ on December 29, 2020

anionic surfactants at the oil-water interface (*27*). This behavior of hydroxide ions appears to be ubiquitous phenomena in various interfaces between water and hydrophobic media (*28*–*30*). For positively charged MitoTracker, the electrostatic attraction between MitoTracker dyes and negative charges formed at the oil-water interface makes dyes localized near the surface of microdroplets. On the other hand, negatively charged AF647 dyes were repelled by the negative charges at the microdroplet surface.

Next, we imaged microdroplets containing each dye and 100 mM NaCl, a physiologically relevant salt concentration. The positively charged dye molecules, MitoTracker, were still localized at the periphery of the microdroplets (Fig. 1A), whereas the negatively charged dye molecules, AF647, were relocalized at the periphery (Fig. 1B). This observation shows that salt ions make charged molecules localized near the water-oil interface regardless of their charge. Thus, the spatial distribution of negatively charged ions depends strongly on the addition of salt ions. The same behavior was observed for another negatively charged fluorescent dye, Alexa Fluor 555 (AF555; Fig. 1C). With added salt ions, this electrostatic interaction is screened, and hydrophobic interaction between dyes and between dye molecules and the hydrophobic microdroplet surface becomes dominant (*31*), resulting in the localization of molecules at the surface of microdroplets. Several studies showed that hydroxide ions still dominate in charging of the water-hydrophobic interfaces at neutral and alkaline pH in the presence of salt ions at low to moderate concentrations (*28*), indicating that the relocalization was not caused by the salt-induced exclusion of adsorbed anions from water-oil interface. The added salt can induce a "salting-out" process by increasing the interaction between salt ions and water molecules followed by a lesser amount of free water molecules available to solvate solute molecules, resulting in the hydrophobic interaction between solute molecules becoming thermodynamically favorable (*32*). The results show that in the oil-confined water microdroplets we examined, salt ions play a critical role in the spatial distribution of the negatively charged molecules.

We examined whether the observed localization was influenced by lensing effect, i.e., the refraction of fluorescence light at the curved interface between water and oil, which have slightly different refractive indices, 1.515 for immersion oil (Nikon Inc., Japan) and 1.33 for water. The distribution of dyes in a microdroplet with 48-μm diameter containing 1 μM AF647 dyes and 100 mM NaCl was examined with a confocal microscope. The depth of focus was approximately 300 nm. Two cross-sectional images of the microdroplet were taken at 15 μm above and 15 μm below the equator (Fig. 2). If any substantial reflection occurred, spatial distributions of fluorescent dyes at two different imaging planes should differ while fluorescent lights pass through different geometries of the microdroplet. Two images acquired from the upper and the lower hemispheres of the same microdroplet exhibited essentially similar spatial distribution, although overall intensity in the image obtained from the upper plane was attenuated compared to the one from the lower plane. Table S1 presents that the measured peak widths at the 15 μm above and the 15 μm below the equator remain at similar values. These data show that the lensing effect from microdroplets does not significantly distort the observation of the peripheral localization of fluorescent dyes within the diffraction-limited resolution of the confocal microscope.

We also explored a possible optical distortion in microdroplets by imaging a microdroplet that has fluorescent dyes highly localized only at the surface of microdroplets. We prepared reverse micelles that were made of 1-palmitoyl-2-oleoylphosphatidylcholine (POPC). The micelles were dual-stained with lipid-incorporated dyes, 1,1′-dioctadecyl-3,3,3′,3′-tetramethylindocarbocyanine (DiI) and water-soluble AF647 dyes (fig. S2A). Because the DiI dyes are embedded into the POPC layer, the physical thickness of the dye layer is within a few nanometers. We imaged the stained reverse micelles using the confocal microscope. Figure S2 (B and C) shows the fluorescence images of DiI (green) and AF647 (red) dyes in a microdroplet containing 150 mM NaCl. Fluorescence imaging of DiI dyes in the micelle (fig. S2B) shows that DiI dyes are localized within a full width at half maximum peak width approximately 550 nm (fig. S2C). These data show that the dye locations can be accurately determined within the diffraction-limited resolution of the currently used confocal microscope and that the optical distortion was not significant. The localized distribution of AF647 dyes near the periphery of the reverse micelle containing 150 mM NaCl (fig. S2, B and C) shows that the localization behavior can also be observable in water microdroplets interfacing with phospholipids, which is a dominant interface in cells.

The quantum yield of fluorescent dyes that can undergo cis-trans photoisomerization upon excitation increases as the viscosity of the solution increases (*33*). The local viscosity of water changes at the water-hydrophobic surface (*34*). These suggest that the increased fluorescence intensity of dyes near the water-oil interface might be caused by the increase in the quantum yields of dyes rather than the physical localization of dyes. We examined this possibility by imaging Cy3B dyes that have locked conformation due to the rigid linker between chromophores (fig. S3A). Figure S3 (B and C) shows the fluorescence image and the distribution of Cy3B dyes in a water-in-oil microdroplet. The same localization behavior was observed for the Cy3B dyes, showing that the increased fluorescence intensity at the microdroplet periphery is caused by the localization of dyes, not high viscosity-induced quantum yield increase.

It has been reported that the aqueous microdroplet surface has a different pH compared to bulk water (*35*). We explored whether the localized fluorescence intensity was caused by the increased quantum yield or fluorescence emission spectral change. Figure S4A presents the spectra of AF647 in bulk water with different pH, showing that the fluorescence emission was essentially unchanged over various pH. We also confirmed that the fluorescence spectrum of AF647 dyes did not substantially change under NaCl concentration up to 1 M. These results show that the increased fluorescence of dyes near the periphery of microdroplets was not related to the fluorescence spectral changes caused by pH shift and added salts.

Peripheral localization of biological molecules in microdroplets

Many biological molecules in cells are negatively charged. In particular, nucleic acids such as DNA and RNA are highly negatively charged. We tested whether salt ions can induce the relocalization of negatively charged DNA molecules in water-in-oil microdroplets. For this purpose, we used double-stranded DNAs with lengths of 10 and 30 base pairs (bp) tagged with AF647, which we designate as 10- and 30-bp DNA-AF647, respectively. In microdroplets with no salt ions, 10-bp DNA-AF647 was evenly distributed for the most part with a slight tendency toward peripheral localization (Fig. 1D). However, as in the case of AF647 and AF555, in the presence of 100 mM salt ions, most of 10-bp DNA-AF647 molecules were relocalized

Downloaded from http://advances.sciencemag.org/ on December 29, 2020

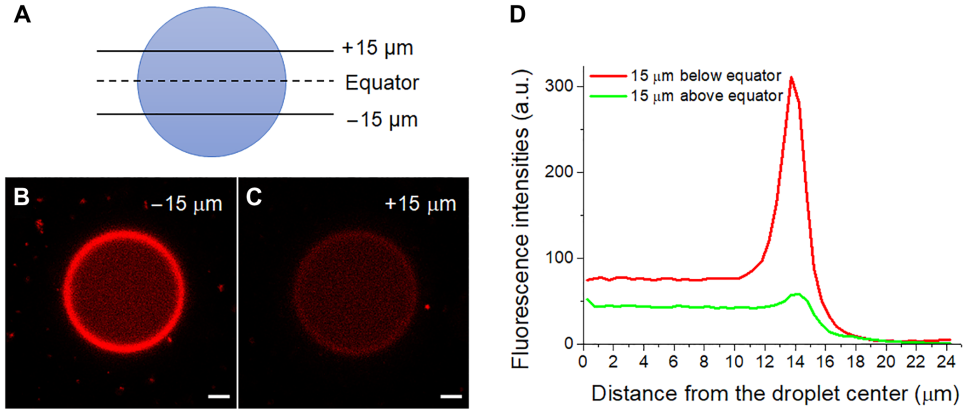

Fig. 2. Spatial distribution of AF647 fluorescent dye at two different cross-sectional planes of the microdroplet (48 μm in diameter). (**A**) Schematic of imaging conditions. (**B** and **C**) Fluorescence images acquired at the 15 μm below (left) and 15 μm above (right) the equator of the microdroplet. (**D**) Distributions of AF647 dyes at the two different imaging planes of the microdroplet. a.u., arbitrary units.

toward the periphery. The 30-bp DNA-AF647 molecules in microdroplets with no salt ions showed a higher tendency for peripheral localization than 10-bp DNA-AF647, but the peripheral localization was still more pronounced with 100 mM NaCl (Fig. 1E).

We further examined the distribution of AF647, AF555, and 10- and 30-bp DNA-AF647 under increasing NaCl concentrations from 0 to 100 mM. Figure 3 shows plots of the average fluorescence intensity as a function of normalized distance from the center to the boundary of a microdroplet. These data revealed that the peripheral localization of all these negatively charged molecules was clearly enhanced with increasing salt concentration. For all the molecules, the localization at the periphery of microdroplets was accompanied by depletion in the inner region of microdroplets, showing that the observed localization at the periphery was caused by salt-induced migration of molecules from the inner region, not caused by the quenching or the enhancement of fluorescence. Notably, the sensitivity to salt concentration for peripheral relocalization depends on the type of molecule. We speculate that the possession of different hydrophilic and hydrophobic domains of each molecule and their availability for interacting with water molecules and salt ions may be responsible for this behavior.

Dependence of salt-induced relocalization on the microdroplet size

We examined the effect of droplet size on salt-induced relocalization using AF647 dye–containing microdroplets with different diameters ranging from 7 to 28 μm (Fig. 4A). Without salt ions, these dyes were nearly evenly distributed in the interior of microdroplets and were depleted from the periphery of microdroplets for all the sizes of microdroplets. It is noteworthy that the slope of dye depletion toward the oil-water interface becomes steeper for smaller microdroplets, suggesting a higher density of negative charges formed at the oil-water interface for smaller microdroplets possibly caused by the increased curvature, which facilitated charge accumulation at the interface. In the presence of 100 mM salt, the relocalization of AF647 dye molecules was highly dependent on the size of microdroplets. In a water-in-oil microdroplet with 7-μm diameter, AF647 dye molecules exhibited a clear relocalization to the periphery with a nearly uniform distribution in the interior. In a microdroplet with 14-μm diameter, the trend was similar but showed a lower peripheral peak than a 7-μm-diameter microdroplet. In microdroplets with 24- and 28-μm diameter, dyes showed a relatively distinctive peripheral peak and a clear presence of a trough before the peripheral peak (Fig. 4A). It thus appears that in larger microdroplets, the relocalization occurs by the migration of molecules from adjacent inner region to the oil-water interface. Thus, it is the distinctive property of the microdroplet with 7-μm diameter, among those we tested, that the salt-induced relocalization effect manifests into the interior part of the microdroplets. Because a typical cellular length scale is approximately 7 μm or less, and aqueous intracellular solution is surrounded by hydrophobic lipids, the observed behavior of salt-induced localization in a water-in-oil microdroplet is expected to reflect biomolecular spatial distribution and localization in cells.

Comparison of dye distribution between water microdroplets and bulk water

We compared the distribution of dyes between water microdroplets to that of the bulk water-oil interface. Figure S1B shows the schematic of the setup for the bulk water-oil interface imaging. Figure 4B shows the fluorescence images of AF647 dye molecules near the bulk water to the bulk oil interface (top panel) and their distribution profiles (bottom panel) with increasing concentrations of NaCl. When no salt was added, AF647 molecules were nearly uniformly distributed in the interior of bulk water but with a gradual depletion near the periphery of the interface, which was similar to the case of larger microdroplets (Fig. 4). At 0.1 mM NaCl concentration, the distribution was essentially unaffected. AF647 dye molecules started migrating toward the boundary at 1 mM NaCl concentration and exhibited a localized distribution near the boundary at 10 mM. At 100 mM NaCl concentration, AF647 showed a noticeable localization peak at the periphery, as in larger microdroplets (Fig. 4A). By contrast, the addition of salt at as little as 0.1 to 1 mM induced the relocalization of AF647 in microdroplets (Fig. 3, B and C). These data indicate that water-in-oil microdroplets provide a higher salt sensitivity for the relocalization of the negatively charged molecule than bulk solution, implying that in the intracellular aqueous phase, the effect of salt ion on molecular localization in microdroplets is more significant than that in bulk solution. We speculate that this behavior might be caused by preferred accumulation of salt ions at the

Downloaded from http://advances.sciencemag.org/ on December 29, 2020

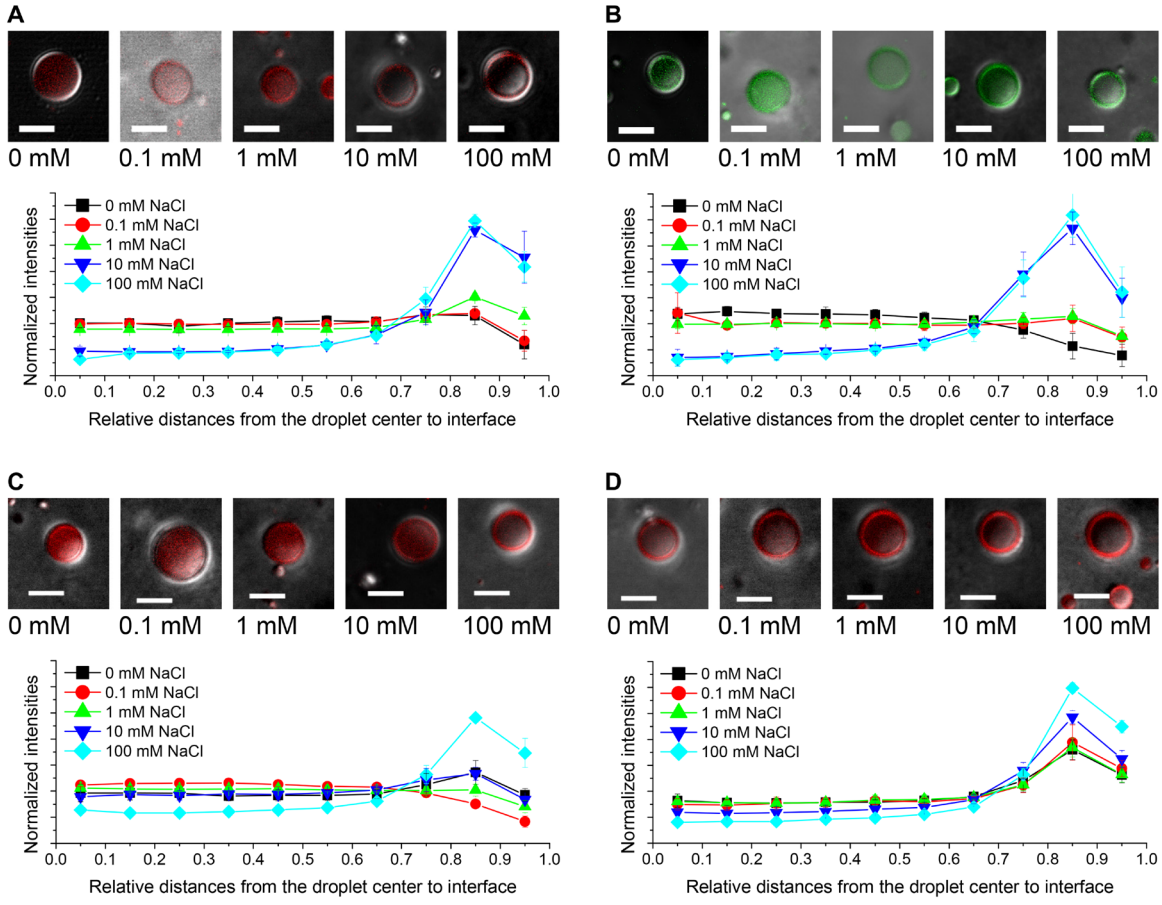

Fig. 3. Effect of different NaCl concentrations on the localization of negatively charged fluorescent dye molecules and DNA molecules tagged with AF647. The fluorescence/bright-field overlay images of aqueous microdroplets containing AF647 (**A**), AF555 (**B**), 10-bp DNA-AF647 (**C**), and 30-bp DNA-AF647 (**D**) with the indicated NaCl concentrations (scale bars, 5 μm). The normalized spatial distributions of each dye under various NaCl concentrations are plotted in the bottom panel. Because different sizes of microdroplets were analyzed, the distance from the center to the boundary of each microdroplet was normalized to one and divided into 10 segments. Fluorescence intensity was averaged in each segment and plotted as a function of the relative distance from the center to the periphery of microdroplets. Error bars represent 1 SD from five independent measurements.

water-oil interface of microdroplets (*36*–*38*), which might facilitate the relocalization through the charge shielding effect (*31*) and salting-out effect (*32*).

Heterogeneous localization behavior of dyes at different oil-water interfaces

Aqueous solution inside biological cells surrounded by various types of hydrophobic molecules mostly includes various lipid molecules. We thus examined the localization behavior of AF647 in aqueous microdroplets that are interfaced with three different hydrophobic oils: glyceryl trioleate (triolein), olive oil, and silicone oil. Figure 5 shows overlays of fluorescence and bright-field images of aqueous microdroplets confined in these oils with diameters less than 10 μm (Fig. 5, A, C, and E) and in bulk aqueous water interfaced with these oils (Fig. 5, B, D, and F). We found that the salt sensitivity for relocalization was markedly different for different oils. The salt sensitivity decreased in the order of silicone oil (Fig. 5, E and F), triolein (Fig. 5, A and B), the immersion oil (Figs. 2A and 3B), and olive oil (Fig. 5, C and D) in both microdroplets and bulk water. The salt sensitivity was again higher in oil-confined microdroplets than in bulk water, as observed in 1 mM NaCl for triolein and silicone oil and in 100 mM for olive oil. These results imply that, in addition to salt concentrations and space dimensions, different hydrophobic interfaces have different effects on the molecular distribution of charged molecules inside cells.

To examine a possible interference on the dye fluorescence intensity by the contact or vicinity to high refractive indices of oils, we compared relative fluorescence intensities of dyes, including AF647 and rhodamine 6G dyes, at the bulk or microdroplet water interfacing with oils that have different refractive indices with and without added NaCl (100 mM) (fig. S5). There was no clear correlation between refractive indices of oils [Fluorinert™ FC-40 (CAS no. 86508-42-1) FC-40, n = 1.29; silicone oil, n = 1.4; olive oil, n = 1.455; triolein oil, n = 1.47; and immersion oil, n = 1.515] and relative fluorescence intensities. These data show that the change in the fluorescence intensity at the microdroplet interface is not caused by the contact with oils that have high refractive indices or from refractive index mismatches. In addition, a previous study reported the localization of the positively charged dye, rhodamine 6G, in water microdroplets in FC-40 (*14*), which shows that the localization behavior is consistently observed in water microdroplets interfacing with different types of oils such as perfluorinated oil.

Downloaded from http://advances.sciencemag.org/ on December 29, 2020

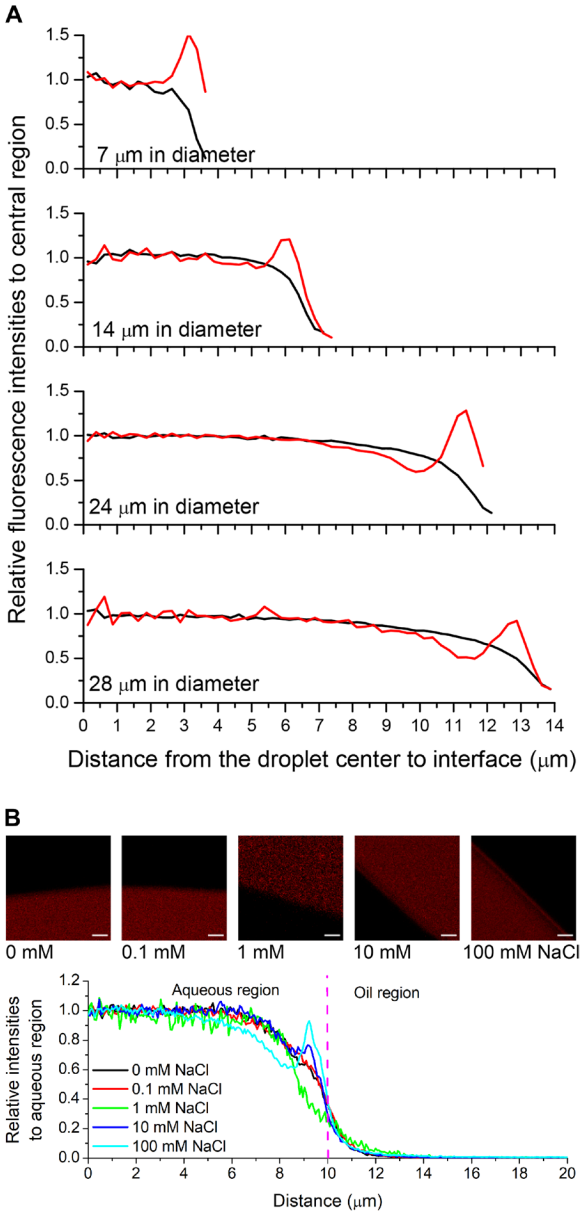

Fig. 4. Different spatial distribution of fluorescent dye in microdroplets and bulk solution. (**A**) Spatial distribution of the fluorescent dye, AF647, in aqueous microdroplets larger than 7 μm in diameter in the absence (black lines) and the presence of 100 mM NaCl (red lines). The microdroplets were interfaced to the immersion oil. The relative fluorescence intensities were plotted against the distances from the droplet center to the interface. (**B**) Spatial distribution of fluorescent dye, AF647, in bulk water containing different salt concentrations from 0 to 100 mM NaCl, which is in contact with immersion oil. Each fluorescence image was recorded on the parallel section above the cover glass by 4.8 μm to avoid the interfering fluorescence signals on the cover glass surface (scale bars, 5 μm). The fluorescence intensities at the interfacial region were plotted against the distance from the interior aqueous part to the oil part, and the contact boundary was marked by the dashed magenta line.

Dependence of salt-induced relocalization on the type of salt cations

Different types of salt ions have distinct effects on various aspects of biochemical reactions, including protein stability, folding, and enzymatic activity (*39*). We thus examined the effect of different cationic species on the localization of AF647 in water microdroplets enclosed in immersion oil. We plotted the fraction of fluorescence intensity of AF647 at the periphery of microdroplets (>70% of microdroplet radius) as a function of salt concentration for different cationic species resulting from the addition of NaCl, KCl, and NH_4Cl (Fig. 6). The fraction of fluorescence intensity localized at the periphery of microdroplets increased with increasing salt concentration and reached a saturating value at 10 mM for all three cation types. These data indicate that salt-induced relocalization of negatively charged dyes is independent of the type of singly charged cations. We also investigated the effect of different types of anionic species on relocalization. However, the relationship between anion types and dye relocalization could not be established because of the strong influence of the anions on the dye fluorescence intensity. Several previous studies show the pH dependence of the zeta potential is independent of the counteranion, including chloride, iodide, or perchlorate, indicating that these anions do not compete with hydroxide or unknown anionic surfactants adsorbed at the water-hydrophobic interface (*29*, *40*).

It was reported that charged molecules were distributed in the interior of water-in-oil microdroplets in the presence of 100 mM salt or buffers (*41*). This behavior may be caused by the influence of added surfactants to the microdroplet interface for stabilizing droplets. We examined this hypothesis by imaging water microdroplets containing AF647 dyes in immersion oil, which have surfactants, SDS, at the water-oil interface (fig. S6A). Figure S6 (B and C) shows fluorescence and bright-field images and distribution of AF647 dyes in microdroplets with the surfactant under different NaCl concentrations up to 100 mM. Both in microdroplet with and without added NaCl, dyes were depleted from the interface and resided in the interior of microdroplets. This observation seems to be caused by the electrostatic repulsion between the negative charge of SDS at the interface and the negative charge of AF657. This result suggests that, when charged surfactants are introduced at the microdroplet, the electrostatic effect becomes dominant over the hydrostatic interaction, and the added salt up to 100 mM was unable to screen completely the electrostatic interaction. These observations suggest that the hydrophobic interaction between water-soluble molecules and hydrophobic media may not be the universal mechanism that elucidates the salt-induced distribution of dyes in microdroplets; instead, combined effects from several mechanisms are involved, particularly when external charged species such as surfactants are introduced at the interface. The detailed picture including salt-water and salt-solute interaction, microscopic distribution of salt ions near the interface, and the electrostatic interaction needs to be further investigated to acquire a comprehensive picture of molecular distributions in geometrically confined water.

CONCLUSIONS

We report that salt ions induce localization of charged molecules in microdroplets. Key findings of this study include the following: (i) Salt ions induce relocalization of negatively charged molecules including DNA from the interior toward the periphery of small aqueous microdroplets confined in oil; (ii) decreasing microdroplet size causes higher sensitivity of the salt-induced relocalization; and (iii) different oil-water interfaces exert different salt sensitivities on molecular relocalization.

Downloaded from http://advances.sciencemag.org/ on December 29, 2020

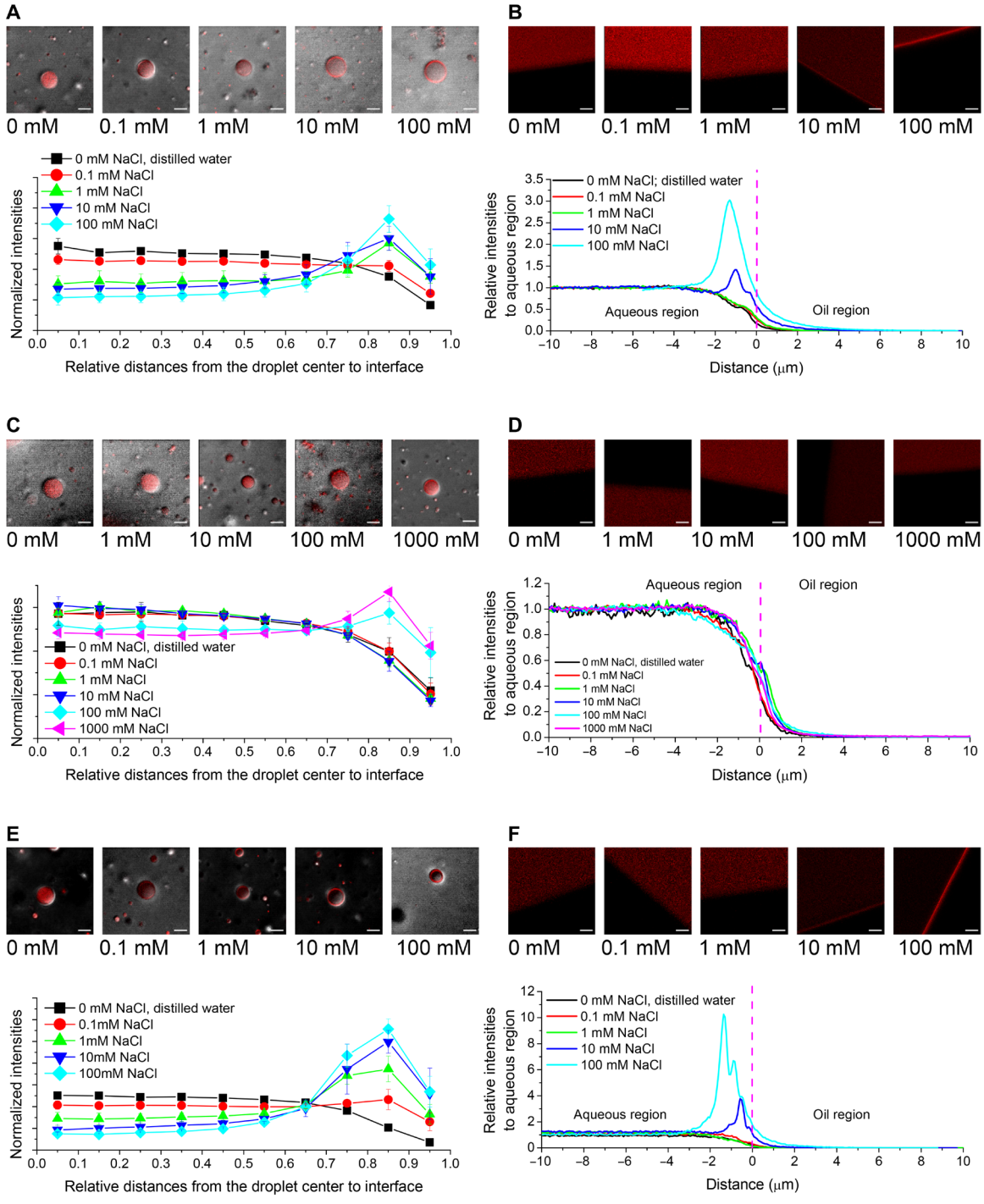

Fig. 5. Spatial localization of dyes for various oil-water interfaces. The changes in the molecular localization of AF647 under various NaCl concentrations when interfacing with different hydrophobic oils; triolein (**A** and **B**), olive oil (**C** and **D**), and silicone oil (**E** and **F**). Overlay of fluorescence and bright-field images and their distribution profiles of AF647 in microdroplets surrounded by each oil (A, C, and E) and fluorescence images near the interface between bulk oil and bulk water (B, D, and F) containing different concentrations of NaCl (scale bars, 5 μm). Error bars represent 1 SD from five independent measurements.

These findings show how charged molecules behave in confined environments at micrometer-sized reaction vessels enclosed by a hydrophobe and how the addition of salt ions influences the distribution of molecules. These also provide an important foundation for accelerated reaction rates observed in microdroplets, and a useful method for enriching the concentration of molecules, consequently, promotes rates of chemical reactions.

In addition, the oil-confined aqueous microdroplets reflect, at least in part, the aqueous environment of a cell where a micrometer-sized aqueous solution is confined by various hydrophobic interfaces,

Downloaded from http://advances.sciencemag.org/ on December 29, 2020

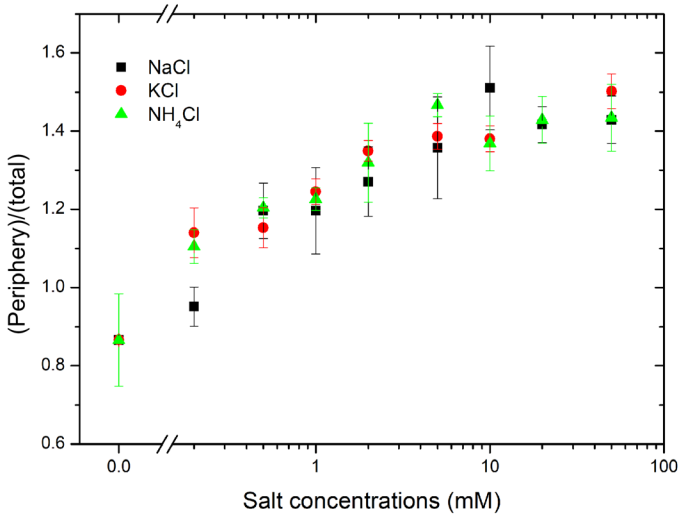

Fig. 6. Effect of different types of cations on the peripheral localization of AF647 in microdroplets. The "Periphery" region is defined as the region where the radius is more than 70% of the whole radius of each droplet. The average fluorescence intensities in the Periphery are compared with those in the whole droplet regions; the value 1.0 reflects that the fluorescent dyes are evenly distributed in the microdroplet including the periphery. Error bars represent 1 SD from five independent measurements.

which contains charged molecules such as amino acids and various metabolites as well as salt ions at concentrations more than 100 mM. Thus, our findings may provide relevant implications for the localization of negatively charged molecules inside cells. The salt ions in cells may influence the localization of charged biomolecules near hydrophobic surfaces of cells and, consequently, change the behaviors of biochemical reactions in cells. Overall, our findings suggest that the biochemical reactions inside cells would be vastly different from those in bulk water solutions.

MATERIALS AND METHODS

Materials

All the fluorescence materials were purchased from Thermo Fisher Scientific (Waltham, MA). The fluorescence-tagged oligomers whose sequences are 5′-AF647-GTGATCATGA-3′ and 5′-AF647-GCGTTGAGCATTGTGCACACGTACACGACT-3′ for 10 and 30 nucleotides, respectively, were acquired from Integrated DNA Technologies (Coralville, IO) who synthesized each sequence. To prepare double-stranded DNA fragments, the complementary oligomers were synthesized and annealed to the fluorescence-tagged DNA oligomers.

Imaging of microdroplets and image analysis

To prepare water-in-oil microdroplets, microfuge tubes containing 10:1 mixture of oil:aqueous solution containing each 1 μM fluorescence dye were placed in a bath sonicator (Elmasonic S 10; Elma Schmidbauer GmbH, Germany) and sonicated for 2 min at "sweep" function in room temperature. Because microdroplets formed by the sonication started fusing after 10 min, confocal images of microdroplets were taken within 10 min so that we could get the images of desirable sized microdroplets ranging from a few to tens of micrometers in diameter and avoid the fusion of microdroplets. Different types of oils were used, including immersion oil [type A; 1,4-dimethyl-2-(1-phenylethyl)benzene; Nikon Inc., Japan], triolein oil [glyceryl trioleate; CAS (Chemical Abstract Service) no. 122-32-7, Sigma-Aldrich, MO], olive oil (CAS no. 8001-25-0, Sigma-Aldrich, MO), or silicone oil (CAS no. 63148-52-7, Sigma-Aldrich, MO). The prepared oil solution emulsion was cast onto a glass slide and imaged with a confocal microscope (LSM 780; Carl Zeiss, GmbH, Germany). The fluorescence signals were recorded with excitation laser beams (561 nm for AF555 and MitoTracker and 633 nm for AF647) and their preprogrammed emission windows. The acquired images were processed with ZEN software suite (Carl Zeiss GmbH, Germany) and ImageJ software (National Institutes of Health, Bethesda, MD). The size of droplet ranged from 3 to 24 μm in diameter. The fluorescence intensities of the observed microdroplets were numerated in terms of pixels, and their positional information was transformed in polar coordinates so that we can present them in distances from the center of the droplet.

Images were taken for water microdroplets freely floating in oil at least 10 μm above the glass surface to prevent any interference originated from the glass surface. To minimize the drift of microdroplets while taking images, we waited typically for 1 min until the initial rapid drift caused by mechanical shock of mounting the glass slide onto a microscope stage was stabilized. The total frame time for a 512 × 512 pixel image arranged between 0.78 and 0.97 s. The frame time for a single microdroplet of 5 μm in diameter was approximately ~2.3 ms. In this time frame, no significant drifts were observed, which was confirmed by the lack of isotropic blurring both in bright-field and fluorescence images.

For the preparation of the bulk interface between water and oil, we placed the 1 μl of aqueous solution on a cover glass and covered it with a sufficiently large volume of oil. The radius of 1-μl aqueous solution droplet was approximately 782 μm, which was far larger than the sizes of typical microdroplets examined in this study. Then, we took z-section images of the bulk interface that are perpendicular to the glass surface at 4.8 μm above the glass surface to avoid the surface interfering signal.

The effect of pH and the salt concentration on the fluorescence spectrum of AF647 dye molecules were examined by dissolving the dye at the final concentration of 150 nM containing 100 mM sodium phosphate buffer with pH adjusted to 4, 7, and 10; or various NaCl concentrations ranging from 0 mM to 1 M. The fluorescence spectra were acquired using a fluorescence microplate reader (Synergy Neo2; BioTek Instruments, VT) with 625 ± 10–nm excitation beam.

The reverse micelle was prepared by emulsifying POPC-containing oil and aqueous solution. After making dry film of POPC on the bottom of a glass vial under nitrogen gas perfusion, the triolein oil and the DiI stock solution were added to the dry film to make the final concentration of 1 mM POPC and 100 nM DiI. To complete the solvation, the mixture was sonicated for 1 hour at 50°C in the bath sonicator. Then, the 1 μM AF647 in 150 mM NaCl solution was added to the oil mixture with 1:10 ratio. The micelle formation process through a bath sonication is the same as the water-in-oil droplet formation described above.

SUPPLEMENTARY MATERIALS

Supplementary material for this article is available at http://advances.sciencemag.org/cgi/content/full/6/41/eaba0181/DC1

View/request a protocol for this paper from *Bio-protocol*.

Downloaded from http://advances.sciencemag.org/ on December 29, 2020

REFERENCES AND NOTES

1. J. K. Lee, S. Kim, H. G. Nam, R. N. Zare, Microdroplet fusion mass spectrometry for fast reaction kinetics. *Proc. Natl. Acad. Sci. U.S.A.* **112**, 3898–3903 (2015).
2. J. K. Lee, H. G. Nam, R. N. Zare, Microdroplet fusion mass spectrometry: accelerated kinetics of acid-induced chlorophyll demetallation. *Q. Rev. Biophys.* **50**, e2 (2017).
3. A. Fallah-Araghi, K. Meguellati, J.-C. Baret, A. E. Harrak, T. Mangeat, M. Karplus, S. Ladame, C. M. Marques, A. D. Griffiths, Enhanced chemical synthesis at soft interfaces: a universal reaction-adsorption mechanism in microcompartments. *Phys. Rev. Lett.* **112**, 028301 (2014).
4. R. M. Bain, C. J. Pulliam, S. A. Raab, R. G. Cooks, Chemical synthesis accelerated by paper spray: The haloform reaction. *J. Chem. Educ.* **93**, 340–344 (2016).
5. R. M. Bain, C. J. Pulliam, R. G. Cooks, Accelerated Hantzsch electrospray synthesis with temporal control of reaction intermediates. *Chem. Sci.* **6**, 397–401 (2015).
6. X. Yan, R. M. Bain, R. G. Cooks, Organic reactions in microdroplets: reaction acceleration revealed by mass spectrometry. *Angew. Chem. Int. Ed. Eng.* **55**, 12960–12972 (2016).
7. R. Obexer, A. Godina, X. Garrabou, P. R. E. Mittl, D. Baker, A. D. Griffiths, D. Hilvert, Emergence of a catalytic tetrad during evolution of a highly active artificial aldolase. *Nat. Chem.* **9**, 50–56 (2017).
8. S. Banerjee, H. Prakash, S. Mazumdar, Evidence of molecular fragmentation inside the charged droplets produced by electrospray process. *J. Am. Soc. Mass Spectrom.* **22**, 1707–1717 (2011).
9. S. Banerjee, Induction of protein conformational change inside the charged electrospray droplet. *J. Mass Spectrom.* **48**, 193–204 (2013).
10. I. Nam, J. K. Lee, H. G. Nam, R. N. Zare, Abiotic production of sugar phosphates and uridine ribonucleoside in aqueous microdroplets. *Proc. Natl. Acad. Sci. U.S.A.* **114**, 12396–12400 (2017).
11. I. Nam, H. G. Nam, R. N. Zare, Abiotic synthesis of purine and pyrimidine ribonucleosides in aqueous microdroplets. *Proc. Natl. Acad. Sci. U.S.A.* **115**, 36–40 (2018).
12. J. K. Lee, D. Samanta, H. G. Nam, R. N. Zare, Micrometer-sized water droplets induce spontaneous reduction. *J. Am. Chem. Soc.* **141**, 10585–10589 (2019).
13. J. K. Lee, K. L. Walker, H. S. Han, J. Kang, F. B. Prinz, R. M. Waymouth, H. G. Nam, R. N. Zare, Spontaneous generation of hydrogen peroxide from aqueous microdroplets. *Proc. Natl. Acad. Sci.* **116**, 19294–19298 (2019).
14. Z. Zhou, X. Yan, Y. H. Lai, R. N. Zare, Fluorescence polarization anisotropy in microdroplets. *J. Phys. Chem. Lett.* **9**, 2928–2932 (2018).
15. K. Tomobe, E. Yamamoto, D. Kojić, Y. Sato, M. Yasui, K. Yasuoka, Origin of the blueshift of water molecules at interfaces of hydrophilic cyclic compounds. *Sci. Adv.* **3**, e1701400 (2017).
16. J. Grdadolnik, F. Merzel, F. Avbelj, Origin of hydrophobicity and enhanced water hydrogen bond strength near purely hydrophobic solutes. *Proc. Natl. Acad. Sci.* **114**, 322–327 (2017).
17. P. Ball, Water as an active constituent in cell biology. *Chem. Rev.* **108**, 74–108 (2008).
18. J. C. Warren, S. G. Cheatum, Effect of neutral salts on enzyme activity and structure. *Biochemistry* **5**, 1702–1707 (1966).
19. G. Corsaro, Salt and solvent effects on reaction mechanism. *J. Chem. Educ.* **54**, 483 (1977).
20. A. M. Hyde, S. L. Zultanski, J. H. Waldman, Y.-L. Zhong, M. Shevlin, F. Peng, General principles and strategies for salting-out informed by the Hofmeister series. *Org. Process Res. Dev.* **21**, 1355–1370 (2017).
21. F. Hofmeister, About the science of the effects of salts: About the water withdrawing effect of the salts. *Arch. Exp. Pathol. Pharmacol.* **24**, 247–260 (1888).
22. O. Krivosheeva, A. Dedinaite, P. M. Claesson, Salt-and pH-induced desorption: Comparison between non-aggregated and aggregated mussel adhesive protein, Mefp-1, and a synthetic cationic polyelectrolyte. *J. Colloid Interface Sci.* **408**, 82–86 (2013).
23. A. Tiraferri, P. Maroni, M. Borkovec, Adsorption of polyelectrolytes to like-charged substrates induced by multivalent counterions as exemplified by poly (styrene sulfonate) and silica. *Phys. Chem. Chem. Phys.* **17**, 10348–10352 (2015).
24. C.-X. Liu, S.-P. Zhang, Z.-G. Su, P. Wang, Salt induced irreversible protein adsorption with extremely high loadings on electrospun nanofibers. *Langmuir* **27**, 760–765 (2010).
25. A. D. McLaren, The adsorption and reactions of enzymes and proteins on kaolinite. I. *J. Phys. Chem.* **58**, 129–137 (1954).
26. A. Kato, M. Yanagisawa, Y. T. Sato, K. Fujiwara, K. Yoshikawa, Cell-Sized confinement in microspheres accelerates the reaction of gene expression. *Sci. Rep.* **2**, 283 (2012).
27. K. G. Marinova, R. G. Alargova, N. D. Denkov, O. D. Velev, D. N. Petsev, I. B. Ivanov, R. P. Borwankar, Charging of oil–water interfaces due to spontaneous adsorption of hydroxyl ions. *Langmuir* **12**, 2045–2051 (1996).
28. R. Zimmermann, U. Freudenberg, R. Schweiß, D. Küttner, C. Werner, Hydroxide and hydronium ion adsorption—A survey. *Curr. Opin. Colloid Interface Sci.* **15**, 196–202 (2010).
29. J. K. Beattie, A. M. Djerdjev, G. G. Warr, The surface of neat water is basic. *Faraday Discuss.* **141**, 31–39 (2009).
30. C. Bai, J. Herzfeld, Surface propensities of the self-ions of water. *ACS Cent. Sci.* **2**, 225–231 (2016).
31. R. Perez-Jimenez, R. Godoy-Ruiz, B. Ibarra-Molero, J. M. Sanchez-Ruiz, The efficiency of different salts to screen charge interactions in proteins: A Hofmeister effect? *Biophys. J.* **86**, 2414–2429 (2004).
32. W.-H. Xie, W.-Y. Shiu, D. Mackay, A review of the effect of salts on the solubility of organic compounds in seawater. *Mar. Environ. Res.* **44**, 429–444 (1997).
33. S. Sharafy, K. A. Muszkat, Viscosity dependence of fluorescence quantum yields. *J. Am. Chem. Soc.* **93**, 4119–4125 (1971).
34. M. Shaat, Viscosity of water interfaces with hydrophobic nanopores: Application to water flow in carbon nanotubes. *Langmuir* **33**, 12814–12819 (2017).
35. H. Wei, E. P. Vejerano, W. Leng, Q. Huang, M. R. Willner, L. C. Marr, P. J. Vikesland, Aerosol microdroplets exhibit a stable pH gradient. *Proc. Natl. Acad. Sci. U.S.A.* **115**, 7272–7277 (2018).
36. P. Jungwirth, D. J. Tobias. (ACS Publications, 2002).
37. P. B. Petersen, R. J. Saykally, On the nature of ions at the liquid water surface. *Annu. Rev. Phys. Chem.* **57**, 333–364 (2006).
38. S. Dewan, V. Carnevale, A. Bankura, A. Eftekhari-Bafrooei, G. Fiorin, M. L. Klein, E. Borguet, Structure of water at charged interfaces: A molecular dynamics study. *Langmuir* **30**, 8056–8065 (2014).
39. H. I. Okur, J. Hladílková, K. B. Rembert, Y. Cho, J. Heyda, J. Dzubiella, P. S. Cremer, P. Jungwirth, Beyond the Hofmeister series: ion-specific effects on proteins and their biological functions. *J. Phys. Chem. B* **121**, 1997–2014 (2017).
40. J. K. Beattie, A. M. Djerdjev, The pristine oil/water interface: Surfactant-free hydroxide-charged emulsions. *Angew. Chem. Int. Ed.* **43**, 3568–3571 (2004).
41. S. Rahmanseresht, P. Milas, K. P. Ramos, B. D. Gamari, L. S. Goldner, Single-molecule-sensitive fluorescence resonance energy transfer in freely-diffusing attoliter droplets. *Appl. Phys. Lett.* **106**, 194107 (2015).

Acknowledgments: We are grateful to W. Min and H. Xiong, Department of Chemistry, Columbia University, for useful comments. **Funding:** This work was supported by the Institute for Basic Science (IBS-R013-D1) and the Air Force Office of Scientific Research through the Basic Research Initiative grant (AFOSR FA9550-12-1-0400). **Author contributions:** S.L., J.K.L., S.K., R.N.Z., and H.G.N. designed the research. S.L., J.K., Sh. K, and S.K. performed the research. S.L., J.K.L., and J.K. analyzed data. S.L., J.K.L., R.N.Z., and H.G.N. wrote the paper. **Competing interests:** The authors declare that they have no competing interests. **Data and materials availability:** All data needed to evaluate the conclusions in the paper are present in the paper and/or the Supplementary Materials. Additional data related to this paper may be requested from the authors.

Submitted 29 October 2019
Accepted 19 August 2020
Published 7 October 2020
10.1126/sciadv.aba0181

Citation: S. Lhee, J. K. Lee, J. Kang, S. Kato, S. Kim, R. N. Zare, H. G. Nam, Spatial localization of charged molecules by salt ions in oil-confined water microdroplets. *Sci. Adv.* **6**, eaba0181 (2020).

Downloaded from http://advances.sciencemag.org/ on December 29, 2020

Science Advances

Spatial localization of charged molecules by salt ions in oil-confined water microdroplets

SangMoon Lhee, Jae Kyoo Lee, Jooyoun Kang, Shota Kato, Sunhee Kim, Richard N. Zare and Hong Gil Nam

Sci Adv **6** (41), eaba0181.
DOI: 10.1126/sciadv.aba0181

ARTICLE TOOLS http://advances.sciencemag.org/content/6/41/eaba0181

SUPPLEMENTARY MATERIALS http://advances.sciencemag.org/content/suppl/2020/10/05/6.41.eaba0181.DC1

REFERENCES This article cites 40 articles, 7 of which you can access for free
http://advances.sciencemag.org/content/6/41/eaba0181#BIBL

PERMISSIONS http://www.sciencemag.org/help/reprints-and-permissions

Use of this article is subject to the Terms of Service

Science Advances (ISSN 2375-2548) is published by the American Association for the Advancement of Science, 1200 New York Avenue NW, Washington, DC 20005. The title *Science Advances* is a registered trademark of AAAS.

Copyright © 2020 The Authors, some rights reserved; exclusive licensee American Association for the Advancement of Science. No claim to original U.S. Government Works. Distributed under a Creative Commons Attribution NonCommercial License 4.0 (CC BY-NC).

Downloaded from http://advances.sciencemag.org/ on December 29, 2020